Partial-wave dispersion relations for the nonrelativistic five-nucleon system*

M. Stingl†
University of Freiburg, Freiburg, West Germany

A. S. Rinat (Reiner)
Weizmann Institute of Science, Rehovot, Israel

(Received 11 February 1974)

Partial-wave dispersion relations for the coupled $\alpha + n$ and $t + d$ channels of the $Z = 2$ five-nucleon system have been solved by the matrix N/D technique. Driving terms have been constructed from one- and two-cluster exchange graphs with parameters of vertex functions taken from studies of $A \leq 4$ subsystems. Accurate solutions to the coupled N and D equations have been obtained by a Pagels approximation based on $[N, N-1]$ Padé approximants. Coulomb forces in charged-fragment channels were incorporated via the repeated N/D scheme of Kinoshita and Kugler. No proper treatment has been given of the anomalous threshold of the $t + d \to \alpha + n$ proton-exchange graph. Calculated $\alpha + n$ scattering phase shifts lack uniqueness, due to strong sensitivity to the inaccurately known vertex parameters used as input, but display the basic features of repulsion in the s wave, occurrence of resonances in the p waves, and existence of the small $3/2^+$, d-wave resonance just above the $t + d$ threshold. Failure of the calculation to produce the width of the p-wave resonances is attributed to the improper treatment of the anomalous threshold. Differential cross sections for $t + d \to \alpha + n$ show reasonable agreement with experiment in both the forward and backward directions but lack details of the observed structure at medium angles. The latter again occurs for the calculated $t + d$ elastic scattering cross sections which moreover are unsatisfactory at forward angles. A comparison with other coupled-channel calculations of light systems is attempted.

[NUCLEAR REACTIONS ^{4}He$(n,n)^4$He, $E = 0$–40 MeV; calculated $S_{1/2}$ through $D_{3/2}$ phase shifts; ^{3}H(d,n) and ^{3}H(d,d), $E = 6$ and 14.2 MeV; calculated $\sigma(\theta)$. Dispersion-relation method.]

1. INTRODUCTION

The study of few-nucleon systems belongs to a particular branch of nuclear physics. These systems are thought to be simple enough to enable highly accurate and sometimes exact descriptions in terms of a bare nucleon-nucleon interaction. The outstanding example is of course the $A = 3$ system which enjoyed tremendous interest in the past decade. The starting point in this development has been the pioneering work of Faddeev[1] who formulated a mathematically rigorous approach. In its wake an extensive literature bears evidence of the numerous aspects that turned up in the realization of Faddeev's program.

For our purpose we mention two of these. Given the exact Faddeev equations for coupled amplitudes one may try to improve on the input which, for computational reasons, is simpler than what is commonly called "realistic" nuclear information. In the earliest applications for instance one could only handle an input of rather crude rank-one interactions between nucleons, which permitted practical solutions of the Faddeev equations by matrix inversion.[2] Nowadays one applies Padé approximants to local realistic interactions.[3]

More physical aspects emerge from a comparison of a vast body of data on the $A = 3$ system with predictions. The data encompass the binding energy, electromagnetic form factors, angular distributions and polarizations in two-body scattering, complete 3-body breakup data, etc.[4,5] The comparison should amongst other things tell us whether bare three-body forces need be introduced; they may help to determine the relative weight of tensor interactions, etc. Interfering with the credibility of answers to this question, is the sensitivity of predictions to the two-body input, in particular to its off-shell behavior.[6]

Turning now to $A > 3$ systems, there are specific reasons why one would like to be able to tackle these. We mention that (for not too high energies) genuinely different two-body channels occur of course only for $A \geq 4$. Next for $A = 4$ and 5 one encounters for the first time resonances.[7] One may hope that a description of relatively narrow resonances in, e.g., the $A = 5$ systems, starting from a two-nucleon force, will be useful in understanding a universal nuclear phenomenon.

It seems that the five-particle system, i.e., the coupled α-nucleon and d-helion channels, is particularly suited for such a study, on which we report below. The first open channel, α plus nucleon, has no competition below the first in-

elastic threshold at $E_2 \approx 17.6$ MeV. Elastic scattering for $E < E_2$ thus ideally tests the influence of a closed channel on a single open channel, which incidentally has a simple spin-isospin structure. A theory should in particular produce locations and widths of the two lowest p-wave resonances and give a fundamental description of the observed spin-orbit coupling. Of special interest is, further, the $d_{3/2}$ resonance just above E_2. Its position and narrow width are clearly related to the coupling of the elastic with (at least) the $d+t$ channel.

Guided by the success of the Faddeev theory one would attempt to search for generalizations thereof for $A \geq 4$. Only few formulations reached the required level of rigor,[8] but when it comes to applications one encounters enormous computational difficulties. Some exploratory approximations have been worked out[9] but one clearly is still far from a scheme that is both workable and "realistic."

In view of the stated interest in solutions of few-nucleon problems, entirely different approaches have been tried. Roughly speaking these have been of two types, namely variational methods and dispersion techniques. In the first category one finds new applications of the resonating group method as well as use of the Kohn-Hulthén variational principle. Both approaches deal with coupled Schrödinger equations where channel coupling is expressed in terms of bare interactions and wave functions of channel fragments. Successful calculations for $A = 5$ have been reported[10, 11] and we shall return to these in our final discussion.

Dispersion techniques used in nuclear problems have until now been of two types and concentrated respectively on forward elastic[12] and general partial-wave amplitudes.[13, 14] The former application is based on a genuine S-matrix theory and ultimately relates observed total cross sections, the real part of the forward amplitude, pole positions and residues.[12] Forward dispersion relations therefore provide a consistency check on parameters and functions extracted from experiment. In particular their predictive value is limited to one coupling constant, or to a constraint on several ones. Partial-wave dispersion relations as used in high-energy physics also exploit proved or assumed analytic properties of partial wave S-matrix elements.[13, 14] Direct application to scattering problems of nuclear physics would however require the introduction of nonnucleonic degrees of freedom.[15]

We have in the past formulated an alternative approach inspired by the rigorously proved dispersion relations for partial-wave amplitudes in potential scattering from Yukawa-type potentials.[16] In the postulated generalization,[13] coupled partial-wave amplitudes for transitions between two-fragment channels with a total number of particles A are assumed to satisfy some set of coupled-channel equations which, to be sure, contain only nucleonic degrees of freedom and which define an analytic continuation in the energy variable. Again, assumptions about analytic properties are then concisely embodied in coupled partial-wave dispersion relations. These may then be solved by the matrix N/D-factorization method.

In the N/D approach to coupled amplitudes, two features stand out. One is the preservation of two-cluster unitarity, the second the nature of the driving terms. Here (and incidentally in potential theories of the Faddeev type) the emphasis is on effective, renormalized driving terms related to subsystems of $A' < A$ particles, and which allude to what is called the dominant reaction mechanism (nucleon exchange in stripping, etc.). We recall that, in contradistinction, the variational theories employ driving terms expressed in the bare nucleon-nucleon interaction. The few subsystem parameters characterizing renormalized driving terms (vertex parameters) could either be computed from microscopic wave functions or be taken directly from experiment.[17] These parameters may then be said to form the input, much the same as the adjusted parameters of the chosen semiphenomenological two-nucleon force form the input for variational calculations.

We have given in Ref. 13 the outline of a many-channel N/D reaction theory. Basing ourselves on that formulation we shall collect in Sec. 2 the essential concepts and formulae without rederivation. Encouraged by the satisfactory results for the three-nucleon problem[14] we then discuss in Sec. 3 the input for the $A = 5$ problem. Numerical results for n-^{4}He and d-^{3}H elastic scattering and for the $d + {}^3\mathrm{H} \to n + {}^4\mathrm{He}$ stripping reaction are given in Sec. 4. A general discussion, comparison to other approaches, and a conclusion appear in Sec. 5.

2. RESUME OF MULTICHANNEL ND^{-1} EQUATIONS

We start here with a condensed resumé of the ND^{-1} method as adapted to low-energy nuclear reactions, which will, moreover, serve to display our notation and conventions. We follow our presentation in Ref. 13 where we incidentally alluded to modifications necessary to include long-range Coulomb forces acting between charged fragments. These modifications are a straightforward application of the formalism of Ref. 18 and are applied here without rederivation.

Consider a nonrelativistic, A-nucleon system which allows for n_C divisions into asymptotically free pairs of clusters C and an unspecified number of three—or more—cluster divisions. We shall understand C to denote the internal quantum numbers of the two clusters c_1 and c_2 in a particular fragmentation, *except* their spin orientations m_1, m_2, and $\vec{k}_C$ the relative momentum of the two fragments. In the center-of-mass (c.m.) system a specification of an asymptotic state in "channel" C is thus

$$\{C=(c_1, c_2),\ m_1, m_2, \vec{k}_C\}. \tag{2.1}$$

The symbol

$$c_1=\{A_1, Z_1, \epsilon_1, j_1, \pi_1, \ldots\} \tag{2.2}$$

will comprise the nucleon number and charge, A_1 and Z_1, the binding energy $\epsilon_1=-|\epsilon_1|$, spin and parity, and other quantum numbers specifying uniquely the state of c_1. At a center-of-mass energy E

$$k_C=k_C(E)\equiv\frac{1}{\hbar}\left[2M_C(E-E_C)\right]^{1/2}, \tag{2.3}$$

with M_C the reduced masses and $E_C=\epsilon_1+\epsilon_2$, the (ordered) threshold energies of channels C.

The unpolarized differential cross section for a transition between two asymptotic states of type (2.1) equals

$$\frac{d\sigma_{CC'}(E,\Theta)}{d\Omega}=\left(\frac{4\pi^2M_C}{\hbar^2}\right)^2\frac{k_{C'}(E)}{k_C(E)}\frac{1}{(2j_1+1)(2j_2+1)}\sum_{m_1m_2}\sum_{m_1'm_2'}|A_{Cm_1m_2,C'm_1'm_2'}(E+i\epsilon,\vec{k}_C,\vec{k}_{C'})|^2, \tag{2.4}$$

where the c.m. scattering angle is given by $\cos\Theta=(\hat{k}_C\cdot\hat{k}_{C'})$ and where kinematical factors have been chosen so as to give the scattering amplitudes A the dimensions of energy$\times$(length)^3.

We now separate from A the Rutherford amplitude $A^{(\mathrm{Coul})}$ (if $C'=C$) and perform a partial-wave analysis of the remainder, writing

$$\begin{aligned}A_{Cm_1m_2,C'm_1'm_2'}(E+i\epsilon,\vec{k}_C,\vec{k}_{C'})&=\delta_{C'C}\,\delta_{m_1'm_1}\delta_{m_2'm_2}A_C^{(\mathrm{Coul})}(E+i\epsilon,\Theta)\\&+\sum_{J,\pi}(2J+1)\sum_{LSL'S'}\tfrac{1}{2}[1+\pi_1\pi_2\pi_1'\pi_2'(-)^{L+L'}\pi]\,[k_C(E)^L d_{C,L}^{-1}(E+i\epsilon)\\&\times\bar{A}^{J\pi}_{CLS,C'L'S'}(E+i\epsilon)\,d_{C'L'}^{-1}(E+i\epsilon)k_{C'}(E)^{L'}]\,X^{J\pi}_{m_1m_2LS,L'S'm_1'm_2'}(\hat{k}_C,\hat{k}_{C'}).\end{aligned} \tag{2.5}$$

In (2.5) J and π refer to the total angular momentum and parity of the system and S and L to the channel spin and relative orbital angular momentum in C. We further used the general spin-angle functions

$$\begin{aligned}X^{J\pi}_{m_1m_2LS,L'S'm_1'm_2'}(\hat{k}_C,\hat{k}_{C'})&=(-)^{2J+L+L'+S+S'}(-)^{j_1+j_1'-j_2-j_2'+m_1+m_1'+m_2+m_2'}\tfrac{1}{4}[1+\pi_1\pi_2(-)^L\pi][1+\pi_1'\pi_2'(-)^{L'}\pi]\\&\times[(2S+1)(2S'+1)]^{1/2}\sum_{M_J}\sum_{MM'}\sum_{\Sigma\Sigma'}\begin{pmatrix}j_1&j_2&S\\m_1&m_2&-\Sigma\end{pmatrix}\begin{pmatrix}j_1'&j_2'&S'\\m_1'&m_2'&-\Sigma'\end{pmatrix}\\&\times\begin{pmatrix}L&S&J\\M&\Sigma&-M_J\end{pmatrix}\begin{pmatrix}L'&S'&J\\M'&\Sigma'&-M_J\end{pmatrix}Y_{LM}(\hat{k}_C)Y^*_{L'M'}(\hat{k}_{C'}).\end{aligned} \tag{2.6}$$

The partial-wave amplitudes in (2.5) contain specific kinematical and Coulomb singularities[18] which are made explicit by threshold factors $(k_C)^L$ and inverse Coulomb Jost functions,

$$d_{C,L}(E+i\epsilon)=\frac{\Gamma(L+1)}{|\Gamma(L+1+i\eta_C(E))|}\,e^{-i\sigma_{C,L}(E)}. \tag{2.7}$$

Here η_C and $\sigma_{C,L}$ denote the usual Coulomb parameter and Coulomb phase shift. For any complex energy z, the "reduced" partial-wave amplitude matrices $\bar{A}^{J\pi}$ may then be assumed to be real analytic,

$$\bar{A}_{\alpha,\beta}(z^*)=[\bar{A}_{\alpha,\beta}(z)]^*. \tag{2.8}$$

For economy of notation, we shall henceforth concentrate on a certain subspace (J,π) and write the amplitudes as $\bar{A}_{\alpha\beta}(=\bar{A}^{J\pi}_{\alpha\beta})$, where, e.g.,

$$\alpha=\{C, L, S\} \tag{2.9}$$

counts the "subchannels" belonging to that subspace. (Depending on fragment spins j_i, the num-

ber $n_{J\pi}$ of those will generally be larger than just n_C.) We may then state further relevant properties of $\bar{A}$ such as

$$\bar{A}_{\alpha,\beta}(z)=\bar{A}_{\beta,\alpha}(z), \tag{2.10}$$

a consequence of time-reversal symmetry. We finally need a statement on the *singularity structure* of $\bar{A}_{\alpha\beta}$ in the complex z plane. We assume the existence of the usual right-hand or unitarity cuts starting from thresholds E_C and of bound-state poles on the real axis below the first threshold. Further, we postulate interaction or left-hand discontinuities $\mathrm{Im}\bar{B}_{\alpha\beta}(E+i\epsilon)$, located in general on an interval

$$E=-\infty\cdots\Lambda_{CC'}\leq \mathrm{Min}(E_C, E_{C'}) \tag{2.11}$$

along the real axis. The discontinuity of an amplitude $\bar{A}_{\alpha\beta}(z)$ across its cuts is then given by $(2i)^{-1}$ times

$$\mathrm{Im}\bar{A}_{\alpha\beta}=\mathrm{Im}\bar{B}_{\alpha\beta}-\pi\sum_{\gamma}\bar{A}^{*}_{\alpha\gamma}\bar{\rho}_{\gamma}\bar{A}_{\gamma\beta}+\bar{F}_{\alpha\beta}, \tag{2.12}$$

omitting everywhere arguments $E+i\epsilon$. Here $\bar{\rho}$ contains threshold- and Coulomb-modified phase-space factors,

$$\bar{\rho}_{\alpha}(E)\equiv\bar{\rho}_{C,L}(E)=\Theta(E-E_C)\frac{M_C}{\hbar^2}\times[k_C(E)]^{2L+1}|d_{C,L}(E+i\epsilon)|^{-2}, \tag{2.13}$$

while the unitary defect matrix $\bar{F}$ describes the loss of flux into all the fragmentations not included in the selected set of two-cluster channels C. When assumed to decrease sufficiently rapidly as $|z|\to\infty$, amplitudes satisfying (2.12) may be shown[19] to permit a matrix N/D decomposition

$$\bar{A}_{\alpha\beta}(z)=\sum_{\gamma}\bar{N}_{\alpha\gamma}(z)\bar{D}^{-1}{}_{\gamma\beta}(z), \tag{2.14}$$

with the elements of the $\bar{N}$ and $\bar{D}$ matrix functions satisfying linear coupled dispersion relations. We now state the first of the two basic approximations to be adopted throughout this paper, namely

$$\bar{F}_{\alpha\beta}(z)\approx 0 \quad [\text{all } (\alpha,\beta)]. \tag{2.15}$$

It should be emphasized that this neglect of flux losses into nonexplicit channels is not necessary for the ND^{-1} method to work.[20] As shown in Ref. 13, some of these losses (due to three-cluster breakup processes) may even be taken into account approximately without carrying an explicit $\bar{F}$ by using modified phase-space factors $\tilde{\rho}_{\alpha}(E)$ in place of (2.13). However, in the exploratory calculations presented here, we shall strictly keep to Eqs. (2.15) and (2.13) and state the equations expressing our analyticity requirements,

$$\bar{N}_{\alpha\beta}(z)=\bar{B}_{\alpha\beta}(z)-\sum_{\alpha'}\int_{E_{C'}}^{\infty}\frac{(z-E_0)\bar{B}_{\alpha\alpha'}(z)-(E'-E_0)\bar{B}_{\alpha\alpha'}(E')}{z-E'}\bar{\rho}_{\alpha'}(E')\bar{N}_{\alpha'\beta}(E')dE', \tag{2.14a}$$

$$\bar{D}_{\alpha\beta}(z)=\delta_{\alpha\beta}+(z-E_0)\int_{E_C}^{\infty}\frac{\bar{\rho}_{\alpha}(E')}{(E'-E_0)(E'-z)}\bar{N}_{\alpha\beta}(E')dE'. \tag{2.14b}$$

In these equations, the symmetric matrix of left-hand spectral integrals

$$\bar{B}_{\alpha\alpha'}(z)=\frac{1}{\pi}\int_{-\infty}^{\Lambda_{CC'}}\frac{\mathrm{Im}\bar{B}_{\alpha\alpha'}(E'+i\epsilon)}{E'-z}dE' \tag{2.16}$$

forms the input, or *driving-force matrix* which contains the specific dynamics of the system under study. Once these dynamics are specified, the set of Eqs. (2.14a) and (2.14b) for $z=E+i\epsilon$, together with Eqs. (2.14) and (2.5), permits the calculation of scattering amplitudes A satisfying unitarity in the restricted space of two-cluster channels.

Before discussing our choice of $\bar{B}$ we mention approximate algebraic solutions invoking so-called pole approximations to some part of the input. We chose a variant due to Pagels.[21] It is based on approximating the spectral integral

$$\bar{R}_{\alpha}(z)\equiv\bar{R}_{C,L}(z,E_p)=\int_{E_C}^{\infty}\frac{\bar{\rho}_{C,L}(E')}{(E'-E_p)^2(E'-z)}dE' \tag{2.17}$$

by a finite sum of poles (that is, a quotient of two polynomials) for z values off the cut of $\bar{R}_{\alpha}(z)$:

$$\bar{R}_{\alpha}(z)\approx\sum_{n=1}^{n_p}\frac{r_{\alpha,n}(E_p)}{z-a_{\alpha,n}(E_p)} \quad (z \text{ not on } E_C\cdots\infty). \tag{2.18}$$

Here E_p is an arbitrary but fixed real energy below the first threshold and which in Pagel's work is set to zero. It should not be confused with the subtraction energy E_0 needed in general to ensure convergence of the dispersion integral (2.14b) for

$\bar{D}$.[19] While results become independent of E_p only for large enough n_p, they are always rigorously independent of E_0[21] so that one is free to choose that value of E_0 for which the solution takes its simplest form, namely, $E_0 = E_p$. We refer the reader to Appendix A for the technical problem of how to determine pole parameters in the approximation (2.17). The explicit solution of (2.14a) and (2.14b) then reads

$$\bar{N}_{\alpha\beta}(z) = \bar{B}_{\alpha\beta}(z) + \sum_{\gamma} \sum_{n=1}^{n_p} r_{\gamma,n}(a_{\gamma,n} - E_p) \frac{(z-E_p)\bar{B}_{\alpha\gamma}(z) - (a_{\gamma n} - E_p)\bar{B}_{\alpha\gamma}(a_{\gamma n})}{z - a_{\gamma n}} \bar{N}_{\gamma\beta}(a_{\gamma n}), \tag{2.19a}$$

$$\bar{D}_{\alpha\beta}(z) = \delta_{\alpha\beta} + (z-E_p)\left[(z-E_p)\bar{R}_{\alpha}(z)\bar{N}_{\alpha\beta}(z) - \sum_{n=1}^{n_p} r_{\alpha n} \frac{(z-E_p)\bar{N}_{\alpha\beta}(z) - (a_{\alpha n} - E_p)\bar{N}_{\alpha\beta}(a_{\alpha n})}{z - a_{\alpha n}}\right], \tag{2.19b}$$

where the real numbers $\bar{N}_{\alpha\beta}(a_{\alpha n})$ are to be determined from the following system of linear equations:

$$\sum_{\alpha' n'} \left(\delta_{CC'}\delta_{LL'}\delta_{nn'} \left\{ \delta_{SS'} - r_{\alpha n}(a_{\alpha n} - E_p)\left[\bar{B}_{\alpha'\alpha}(a_{\alpha n}) + (a_{\alpha n} - E_p)\left(\frac{d\bar{B}_{\alpha'\alpha}}{dz}\right)_{z=a_{\alpha n}}\right] \right\} \right.$$

$$\left. -(1 - \delta_{CC'}\delta_{LL'}\delta_{nn'}) r_{\alpha' n'}(a_{\alpha' n'} - E_p) \frac{(a_{\alpha n} - E_p)\bar{B}_{\alpha'\alpha}(a_{\alpha n}) - (a_{\alpha' n'} - E_p)\bar{B}_{\alpha\alpha'}(a_{\alpha' n'})}{a_{\alpha n} - a_{\alpha' n'}} \right) \bar{N}_{\alpha'\beta}(a_{\alpha' n'}) = \bar{B}_{\beta\alpha}(a_{\alpha n}). \tag{2.20}$$

Two remarks are in order here. First, there is clearly no need in our case to introduce into $\bar{D}$ CDD poles[22] as used in Ref. 18 to cancel approximate bound-state poles coming from the first additive piece of (2.5), since repulsive Coulomb forces do not give rise to bound states. There remains, of course, the possibility of "genuine" CDD poles which in the present work are simply ignored.

Second, inspection of the integrand in (2.17) shows that the threshold factors $(k_C)^{2L+1}$ cause convergence difficulties. The difficulty may be circumvented by assuming $\bar{\rho}_\alpha$ to be cut off smoothly at an energy E_U, large compared to any energy in the problem. We chose

$$\bar{\rho}_\alpha(E) \to \bar{\rho}_\alpha(E)\left[1 - \delta_{L,0} + \left(\frac{E - E_C}{E_U}\right)^L\right]^{-1}. \tag{2.21}$$

Letting $E_U \to \infty$, the quotient elements $\bar{A}_{\alpha\beta}(E + i\epsilon, E_U)$ remain finite in spite of the divergence of both $\bar{N}$ and $\bar{D}$, and one may check on soluble models with pole input that the limit approached is in fact the correction solution. Throughout the calculations described below we have used

$$n_p = 4, \quad E_0 = E_p = -50 \text{ MeV}, \quad E_U = +1 \text{ GeV}, \tag{2.22}$$

energies being counted from the lowest (here the $\alpha + n$) threshold. With this choice, changes in partial-wave amplitudes when shifting E_p, increasing n_p, or increasing E_u, were less than 2% in absolute magnitude in the worst case (the $J^\pi = \frac{3}{2}^-$ $n + \alpha$ elastic amplitude at $E \lesssim 20$ MeV).

3. SELECTION OF DRIVING FORCES FOR $A = 5$

In the introduction we motivated our choice of the $A = 5$, $Z = 2$ system as a first test ground of the N/D approach to light nuclear systems. Taking the threshold energy for $n + {}^4\text{He}$ scattering as $E_1 = 0$ (by choice) only one more two-fragment channel exists, viz. $d + {}^3\text{H}$ with threshold at $E_2 = 17.59$ MeV. All counted we have for $n - {}^4\text{He}$ scattering only $n_{J\pi} = 3, 4$ coupled channels (for $J = \frac{1}{2}$ and $J \geq \frac{3}{2}$, respectively), while, moreover, partial-wave phases are eigen phases.

In order to set up input matrices $\bar{B}$ for this problem, we closely follow Ref. 13, using the idea that transitions between two-fragment channels should at low and medium energies be dominated by left-hand singularities arising from one-cluster exchange diagrams (pole graphs) and from low-order iterations of these. In a coordinate-space language, this roughly corresponds to retaining effective intercluster forces of longest and next-longest range.

There exist four one-cluster exchange (OCE) graphs in our problem which, after projecting out partial waves and putting external momenta to their on-shell values (2.3), form our first-order input $\bar{B}^{(1)}$. Three of them are shown in Fig. 1. The fourth graph, which is a "crossed" graph for Fig. 1(b) and describes $d({}^3\text{H}, n){}^4\text{He}$ stripping through deuteron exchange, has been omitted from the outset since it contains the ${}^4\text{He} \to d + d$ vertex for which parameter determinations are not available. From purely spatial overlap considerations one would expect that vertex to be much weaker than $\alpha \to {}^3\text{He} + n$.

We only give here the unprojected form of such

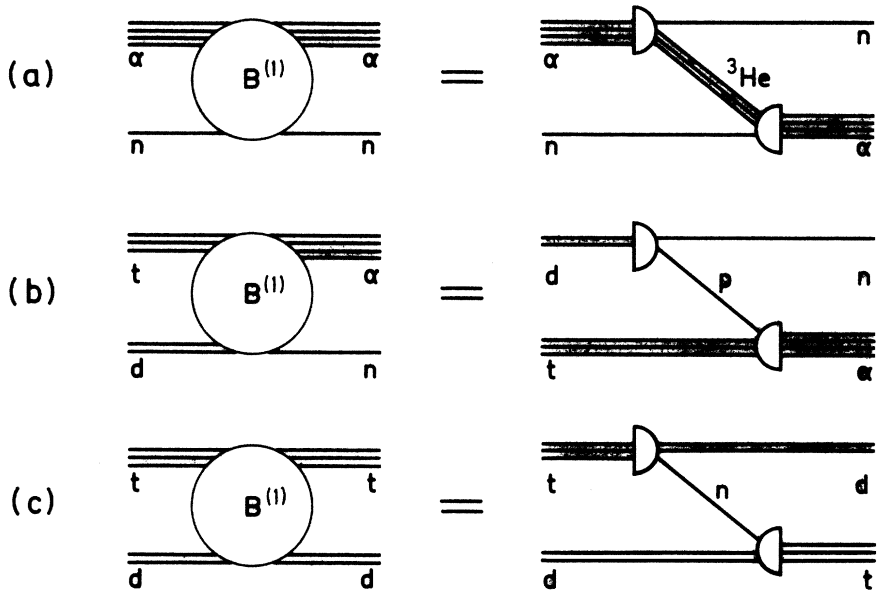

FIG. 1. Pole graphs used to construct first order input matrix $\bar{B}^{(1)}$: (a) for $^4\mathrm{He}+n\rightarrow{}^4\mathrm{He}+n$, (b) for $^3\mathrm{H}+d\rightarrow{}^4\mathrm{He}+n$ (deuteron-exchange graph neglected), (c) for $^3\mathrm{H}+d\rightarrow{}^3\mathrm{H}+d$. Half-circles represent dressed vertex functions.

a graph in a schematical way,

$$\langle\vec{k}\,|\,\bar{B}^{(1)}_{CC'}(E)\,|\,\vec{k}'\rangle=\frac{\Gamma^{1*}_{2'x}(\vec{q})\Gamma^{1'}_{x2}(\vec{q}')}{E-E_{22'x}(\vec{k},\vec{k}')}\,. \tag{3.1}$$

Here x denotes the exchanged cluster, $\Gamma^{1}_{2'x}$ is a vertex function for the virtual breakup of cluster c_1 of channel C into cluster c_2' of channel C' plus cluster x, $E_{22'x}$ is the energy of the intermediate three-cluster state, and $\vec{q}$ and $\vec{q}'$ are the relative momenta in the vertices which through momentum conservation are expressible in terms of the external momenta $\vec{k}$ and $\vec{k}'$.

We shall not repeat here the complete angular-momentum reduction of such a graph for arbitrary spins which we have studied earlier.[23] It finally reduces expression (3.1) to (momentum-space) radial integrals over reduced vertex functions $\tilde{\Gamma}(q)$ which are the partial-wave components of the dressed vertices in Eq. (3.1). In applications, some parametrization is required for these and we adopted throughout the Hulthén form which has correct threshold and asymptotic behavior[24]

$$\tilde{\Gamma}_{a,12}{}^{3}(q,l)=(Zc_a)^{1/2}\tilde{N}_l\cdot\frac{q^l}{(q^2+\beta_l^{\,2})^{l/2+1}}\,. \tag{3.2}$$

In (3.2) q denotes the magnitude of the relative momentum, and l the orbital angular momentum, for fragments 2 and 1 being virtually present in fragment 3. The subscript a denotes antisymmetrized vertices into which we have absorbed the appropriate antisymmetrization factors $c_a{}^{1/2}$ that were still explicit in equations such as (5.5) of Ref. 13.

TABLE I. Parameters of Hulthén vertex functions used in the construction of the driving-force matrix $\bar{B}$.

Vertex	α (fm^{-1})	l	$Z^{1/2}c_a{}^{1/2}\tilde{N}$ (MeV fm$^{-1/2}$)	β (fm^{-1})	$\tilde{g}^2$	Remarks
$d\rightarrow p+n$	0.232	0	48.52	1.313	0.051	$P_S=4\%$
			43.23	1.241		
		2	−81.97	1.528	0.078	$P_D=7\%$
			−194.34	1.948	0.163	
$t\rightarrow d+n$	0.449	0	35.20	1.00	0.172	$C^2\approx 3.4$
			(27···44)	(0.9···1.2)	(0.172···0.25)	(Ref. 26)
$^4\mathrm{He}\rightarrow t+p$	0.846	0	104.20	1.20	2.04	
$^4\mathrm{He}\rightarrow{}^3\mathrm{He}+n$	0.863		(56···141)	(1.1···1.3)	(1.31···2.04)	
$S_{np}\rightarrow p+n$	−0.047	0	arbitrary	1.221	arbitrary	
$S_{nn}\rightarrow n+n$						

We have investigated elsewhere[17] the possibilities of determining such vertex functions from model wave functions or from experimental data for the subsystems. For convenience we summarize in the first eight rows of Table I the strength constants $(Zc_\alpha)^{1/2}\tilde{N}$ and range parameters β_l we have adopted, with minor modifications,[25,26] from Table I of that work. In addition, we entered squared coupling constants[17] $\tilde{g}^2$ and constants α related to the vertex separation energies by

$$\epsilon_1 + \epsilon_2 - \epsilon_3 = \hbar^2\alpha^2/(2\mu_{12}) .$$

Since the choice of input is crucial, we should like to add here a number of comments. While the minus sign of the $l=2$ admixture in the deuteron relative to the $l=0$ part is well established, its magnitude P_D is still uncertain at present.[24] We have therefore adopted from the work of Phillips[24] two parameter sets corresponding to $P_D = 4$ and 7%, respectively, in order to study sensitivity with respect to changes in P_D. On the other hand, an estimate of the $l=2$ admixture in the $^3\mathrm{H} \to d+n$ vertex using realistic ^{3}H and d wave functions[3,27] shows that this component (to be distinguished from the 8–9% D-wave admixture in the ^{3}H wave function) amounts to less than a percent. We therefore neglected this admixture. Finally, we assumed the same parameters for the $^4\mathrm{He} \to {}^3\mathrm{H}+p$ and $^4\mathrm{He} \to {}^3\mathrm{He}+n$ vertices so that Coulomb effects enter only through a different separation energy $\hbar^2\alpha^2/(2\mu)$. Although results on the two different coupling constants have recently become available[28] this simplification seems to us consistent because, as shown in Appendix B, our choice of reduced input $\bar{B}$ anyway amounts to neglecting finer Coulomb effects such as the finite extension and mutual Coulomb polarization of fragment charge distributions.

Parameters for this vertex, as well as for $t \to d+n$, are not very accurately determined at present.[17] Since at the same time these are the parameters to which certain five-nucleon amplitudes are fairly sensitive, we further decided to study the sensitivity by varying the "standard" values of those vertex parameters (rows 5 and 7 of Table I) within certain limits. These limits, which appear in brackets below the standard values, roughly indicate the extent of the present uncertainties. It should be emphasized that we do *not* use these uncertainties for performing any "best fits" to experimental five-nucleon data, since this would contradict the spirit of the theory.

Second-nearest left-hand singularities and the

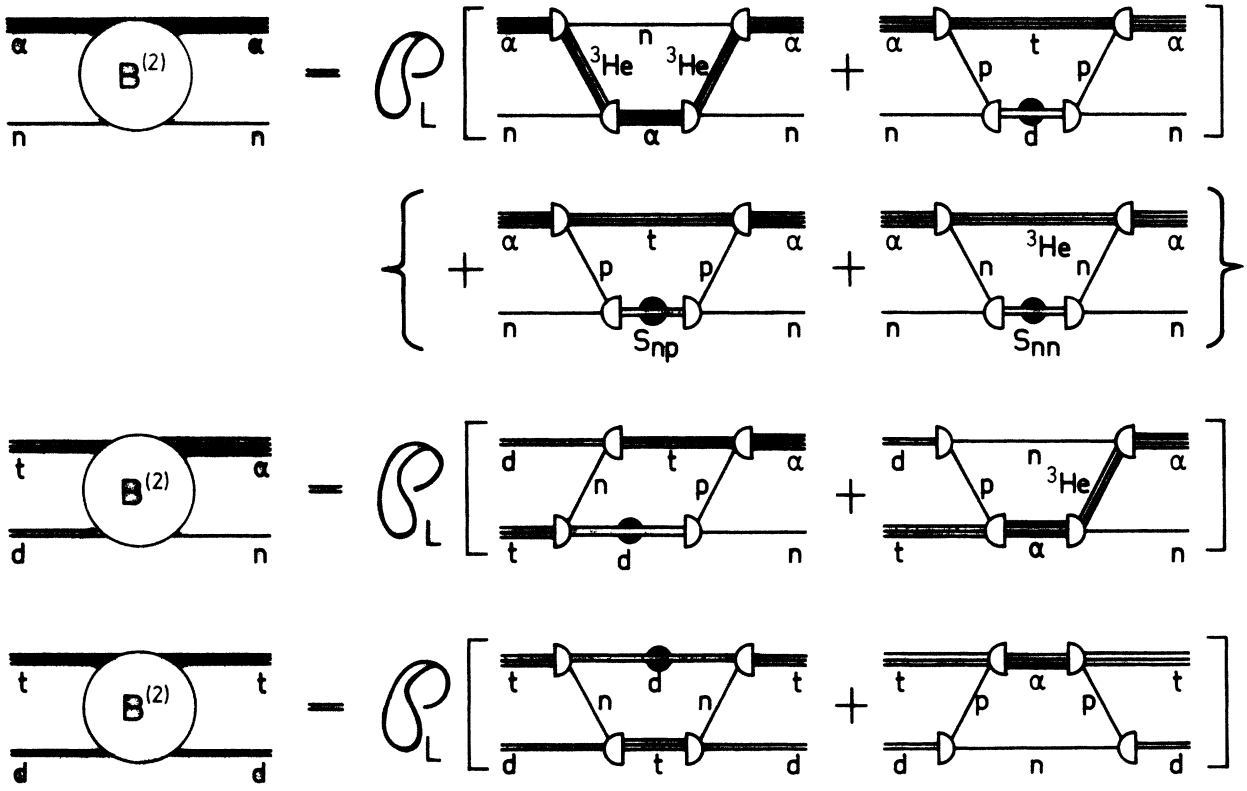

FIG. 2. Once-iterated pole graphs (box graphs) used to construct second order input matrix $\bar{B}^{(2)}$. Black half dots represent dressed propagators.

ensuing driving terms arise, in the framework of the present theory, from once-iterated OCE diagrams which in an off-shell Lippmann-Schwinger formalism[8] represent second Born terms. The relevant graphs for our problem (triangular graphs approximated by box graphs) are depicted in Fig. 2 where the symbol $\mathcal{P}_L$ indicates that left-hand spectral integrals have to be projected out since those graphs in general have also a right-hand cut.

Denoting by $\Omega^{(2)}_{\alpha\beta}(E)$ the second-order Born graph the corresponding driving term free of right-hand singularities is

$$\bar{B}^{(2)}_{\alpha\beta}(E) = \mathcal{P}_L \Omega^{(2)}_{\alpha\beta}(E) = \frac{1}{\pi} \int_L \frac{\mathrm{Im}\Omega^{(2)}_{\alpha\beta}(E')}{E' - E}\, dE' . \tag{3.3}$$

As discussed in Ref. 13, $\bar{B}^{(2)}(E)$ as a repeated Born contribution can be expressed in terms of on-shell and half-off-shell amplitudes $\bar{B}^{(1)}(EE'; E)$:

$$\bar{B}^{(2)}_{\alpha\alpha'}(E) = \sum_{\alpha''} \int_{E_{C''}}^{\infty} \bar{\rho}_{\gamma}(E'') \frac{\bar{B}^{(1)}_{\alpha\alpha''}(E'')\bar{B}^{(1)}_{\alpha''\alpha'}(E'') - \bar{B}^{(1)}_{\alpha\alpha''}(EE'', E)\bar{B}^{(1)}_{\alpha''\alpha'}(E''E, E)}{E'' - E}\, dE'' . \tag{3.4}$$

It is seen from Fig. 2(a) that as intermediate channels C'' in $\bar{B}^{(2)}$ we admit not only $^4\mathrm{He} + n$ and $^3\mathrm{H} + d$ but also the pseudo channels $^3\mathrm{He} + s_{nn}$ and $^3\mathrm{H} + s_{np}$ where the unstable "fragments" s_{nn} and s_{np} are the $^1S_0$ antibound states of the two-neutron and proton-neutron systems. The corresponding vertex parameters are listed in row 9 of Table II. These virtual states are included to simulate the strong nucleon-nucleon interaction in the $^1S_0$ state. It is not possible, at the present level of the theory, to include these pseudo channels as *external* channels, since one must clearly require the answers to be independent of the arbitrary normalization of the $s \to$ nucleon + nucleon vertex—a requirement which in the ND^{-1} formalism can be met only if breakup inelasticities $\bar{F}$ are carried.

A point where we are going slightly beyond the scheme outlined in Ref. 13 is the use of *dressed propagators* in certain intermediate channels. Such dressing may be expected to be important in channels with weakly bound fragments which easily undergo virtual dissociation. We therefore restrict ourselves to dressing, as indicated by the black half circles in Fig. 2, the intermediate two-nucleon systems in a manner familiar from off-shell multiparticle scattering theory,[2,8] which means that we use

$$\tau_C(E' - E) = -\frac{1}{E' - (E + i\epsilon)} \begin{cases} \mathrm{Re}[I_C(E' - E)]^{-1} & (C = {}^3\mathrm{H} + d \text{ or } s) \quad (3.5a) \\ 1 & (C = {}^4\mathrm{He} + n) \quad (3.5b) \end{cases}$$

as propagator for an intermediate system C with total energy $E' = \epsilon_1 + \epsilon_2 + (\hbar^2 k_C{}^2/2M_C)$. Here,

$$I_C(E' - E) = \sum_l \int_0^{\infty} \frac{|2\mu/\hbar^2 \tilde{\Gamma}^{\pi}_{d,11}(q, l)|^2 q^2}{(q^2 + \alpha^2)(q^2 + \gamma^2)}\, dq \begin{pmatrix} \pi = d \\ \text{or } s \end{pmatrix} \tag{3.6}$$

with the abbreviation $\gamma^2 = \alpha^2 + (2\mu/\hbar^2)(E' - E + i\epsilon)$. Again, μ is the reduced mass in the vertex governing the virtual dissociation. Only the real part of the inverse dressing integral is retained in (3.5a) since its imaginary part represents *real* $2 \to 1 + 1$ dissociation and thus contributes to the unitarity defect $\bar{F}$ in (2.12) which we decided to neglect. If we were to carry that imaginary part consistently, we would not only have to apply a matrix ND^{-1} scheme with inelasticities,[20] but also to subtract from our $\bar{B}^{(2)}$ a right-hand spectral integral of that inelasticity. It should therefore be kept in mind that approximation (2.15) also mutilates the input proper to some extent, unless bare propagators are used. Note that for the s pseudo channels, where ϵ_s is on the unphysical sheet and therefore $\alpha = (-2\mu\epsilon_s/\hbar^2 - i0)^{1/2} < 0$, the $+i\epsilon$ in the pole factor of (3.5) is actually superfluous since $I_C{}^{-1}$ vanishes at the pole. This is most directly seen from its explicit expression with the $l = 0$ Hulthén vertex (3.2),

$$I_{^3\mathrm{H}+s}{}^{-1} = \frac{(\alpha + \gamma)(\beta + \gamma)^2}{\alpha(\alpha + \beta)(\alpha + 2\beta + \gamma)} , \tag{3.7}$$

TABLE II. Left-hand branch points $L^{\pm}_{CC'}$ and energies E_R according to Eq. (3.2) for partial-wave projections of the three pole graphs in Fig. 1, the graph of Fig. 1(b) having been replaced by the corresponding "almost anomalous" graph.

Diagram	$L^{-}_{CC'}$ (MeV)	$L^{+}_{CC'}$ (MeV)	E_R (MeV)
Fig. 1(a)	−34.44	−12.35	−18.18
Fig. 1(b)	−68.75	−0.001	−0.10
Fig. 1(c)	−13.82	+16.34	+15.18

where, at $E'=E$, $\gamma=(-2\mu\epsilon_s/\hbar^2+i\epsilon)^{1/2}=-\alpha$. In the approximation (2.15), these propagators then have no imaginary parts at all so that the $\mathcal{P}_L$ may actually be omitted in front of the corresponding $\bar{B}^{(2)}$ graphs. Note also that the over-all constant $Z^{1/2}\tilde{N}$ for the s vertices is arbitrary as required, since in the $^3\mathrm{H}+s$ box graphs there always occurs its absolute square divided by the propagator integral (3.6).

Before closing this section we must comment on a peculiar feature of the amplitude corresponding to the graph in Fig. 1(b) which drives the $^3\mathrm{H}(d,n)$-$^4\mathrm{He}$ transfer in lowest order. This amplitude exhibits an *anomalous threshold,* which is to say that its left-hand cut encircles the lower threshold and continues on an unphysical Riemann sheet[29] as shown schematically in Fig. 3(b). By contrast, a "normal" pole graph has a left-hand cut as in Fig. 3(a), extending between branch points $L^-_{CC'}$ and $L^+_{CC'}$ [cf. Eq. (4.15) of Ref. 13]. Here we are always speaking of the cut arising from the pole propagator, since the additional cuts from the dressed vertex functions $\tilde{\Gamma}$ (the half circles in Fig. 1) are practically always farther to the left and "normal." The anomaly occurs, in a $C \rightleftarrows C'$ pole graph with E_C as lowest threshold, if and only if

$$E_R=\tfrac{1}{2}(E_C+E_{C'})-\frac{1}{2\kappa-1}\tfrac{1}{2}(|\epsilon|+|\epsilon'|)>E_C, \tag{3.8}$$

i.e., if E_R is greater than the lower threshold. Here $\kappa=M_C/\mu'=M_{C'}/\mu$, μ and μ' are the reduced masses and ϵ and ϵ' the binding energies in the two vertices involved. It is seen that an anomalous threshold is generally associated with weak binding in at least one of the vertices. In our example $^3\mathrm{H}$-$(d,n)^4\mathrm{He}$, $\kappa=\frac{8}{5}$ and

$$\begin{aligned}|\epsilon| &= -\epsilon_d = 2.23\ \text{MeV},\\ |\epsilon'| &= \epsilon_{^3\mathrm{H}}-\epsilon_{^4\mathrm{He}} = 19.82\ \text{MeV}.\end{aligned} \tag{3.9}$$

The d binding energy is sufficiently small to give $E_R-E_1=+3.78$ MeV. The "anomaly" entails the following properties. The left-hand and right-hand cuts of the corresponding amplitude are not completely separated, as assumed in the usual ND^{-1} method, and the amplitude develops an inverse-square-root singularity at E_1, in addition to the logarithmic singularity of a normal (partial-wave) pole graph at its upper branch point L^+_{12}. The incorporation of such an anomaly into an Omnès-Mushkelishvili formula for the $1 \rightleftarrows 2$ amplitude has years ago been described by Mandelstam.[30] A proper treatment within a coupled-channel ND^{-1} scheme (where its more complicated effect on the $1 \rightleftarrows 1$ elastic amplitude has to be dealt with simultaneously) is, however, far more difficult and in fact has only recently been worked out in full.[29] Since this treatment inevitably leads to considerable complication of the whole ND^{-1} formalism, and since application of the convenient Pagels's solution is then no more straightforward, we have decided not to delve into this problem at all. Instead we resort to an approximation where the energy $|\epsilon|+|\epsilon'|$ is artificially shifted so as to make the diagram "almost anomalous," that is, to give E_R

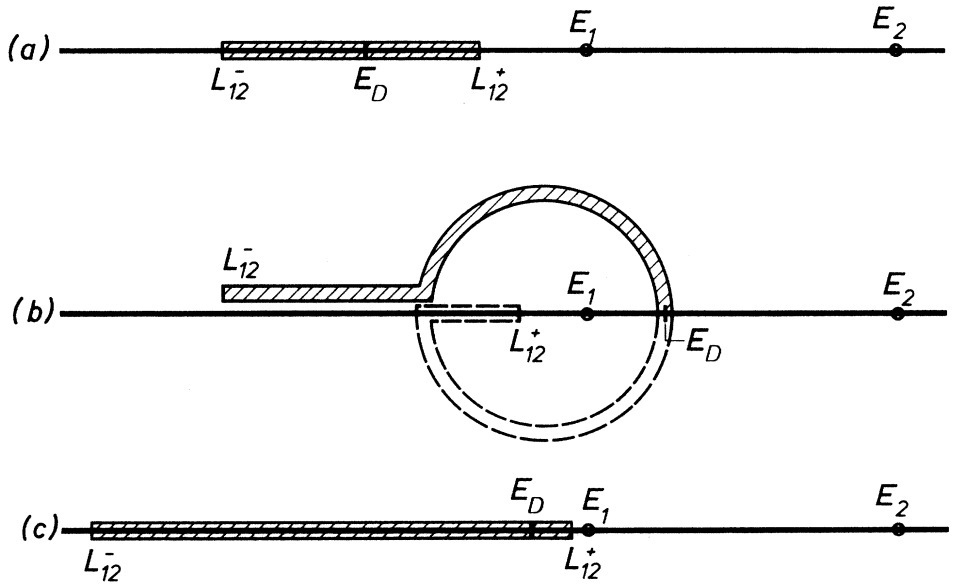

FIG. 3. Location of left-hand cut relative to thresholds E_1 and E_2 for (a) a normal, (b) an anomalous, and (c) the corresponding "almost anomalous" pole graph.

$-E_1$ a small negative value. (The precise value of that quantity is then somewhat arbitrary, but it turns out that taking $E_R - E_1$ anywhere between −0.05 and −5.0 MeV gives about the same results.) Note that the *kinematics* of the graph are left unchanged. This treatment comes to mind because, in the example above, $L_{12}^{-} = -28.66$ MeV and $L_{12}^{+} = -2.42$ MeV, so that the "anomalous section" of the cut is not too large. Still, the procedure results in a considerable shift of the left branch point L_{12}^{-}. This is schematically shown in Fig. 3(c) and numerically in column 2 of Table II where we list the left-hand propagator singularities of the three OCE diagrams actually used. It therefore is possible that we have mutilated the true driving force in a substantial manner, a circumstance that should be kept in mind when discussing α-n scattering, in particular near threshold.

We now summarize our input: (1) Driving forces are used in the approximation

$$\bar{B}(E) \approx \bar{B}^{(1)}(E) + \bar{B}^{(2)}(E), \tag{3.10}$$

which is the second basic approximation of this paper. (2) $\bar{B}^{(1)}$ describes simple exchange, as depicted in Fig. 1 [see Ref. 6, Eqs. (3.15) and (3.17), except that in the present calculation we are not using isospin]. The anomalous threshold is artificially removed. (3) $\bar{B}^{(2)}$ represents the proper part of repeated exchange with the bare propagators $(E'' - E)^{-1}$ of Eq. (3.4) sometimes replaced by the dressed propagators $-\tau_C$ of Eq. (3.5). (4) The vertex parameters for the Γ's in $\bar{B}^{(1)}$ [Eq. (3.1)] are as given in Table I.

4. NUMERICAL RESULTS

In the following we present numerical results obtained by solving Eqs. (2.19) and (2.20), using approximation (2.15) and an input matrix $\bar{B}(E)$ as described in Sec. 3. We discuss below some relevant data and our calculations for the ^{4}He $+n$ scattering phase shifts and the unpolarized ^{3}H $+d \to {}^3$H $+d$ and ^{3}H $+d \to {}^4$He $+n$ angular distributions. Although the general matrix-N/D computer code used in the present calculations produces all the individual m amplitudes (2.5) of the problem, we have in this work abstained from studying any polarization quantities since we expect these to be sensitive to details of vertex angular structure which are either inaccurately known (such as the D admixture in the deuteron) or have been neglected completely (such as the $l=2$ admixture of the $t \to d + n$ vertex).

A. Neutron-α elastic scattering

Experimental data on α-n scattering are summarized in the phase-shift analyses of Arndt and Roper.[31,32] Besides there exist "nuclear" phase shifts for the related charged-particle process ^{4}He$(p,p)^4$He up to $E_p^{\text{c.m.}} \approx 40$ MeV.[32,33] It is to these data that we compare our results in Fig. 4.

For all sets of parameters used, the calculated $S_{1/2}$ phase shift is strongly repulsive as it should be, although always too strong. It also exhibits the observed property that $\delta(\infty) - \delta(0) = -\pi$ in accordance with Swan's extension of the Levinson theorem[34] for elastic scattering from a composite target. In spite of the absence of an $S_{1/2}$ bound state, the phase difference $-\pi$ corresponds to occupancy of an $S_{1/2}$ orbital in the ^{4}He target.

The magnitude of the $S_{1/2}$ phase depends sensitively on both the range and strength constant of the $^4\text{He} \to 3+1$ vertex, so that with the present uncertainty in those parameters no definitive result can be given. The curve of Fig. 4, which was obtained without intermediate s channels and without propagator dressing in $\bar{B}^{(2)}$, and with the "standard" parameter set of Table I, is to be taken as just one example. By varying the $^4\text{He} \to 3+1$ vertex parameters within the limits indicated in row 8 of Table

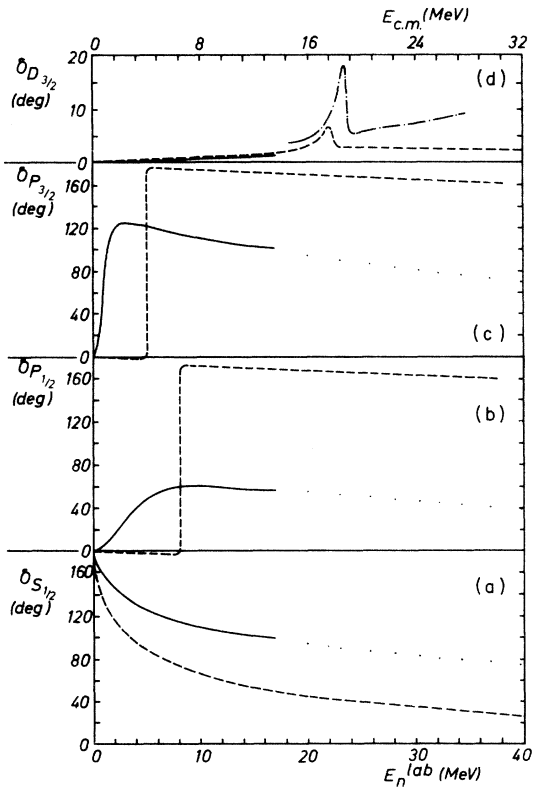

FIG. 4. Phase shifts for ^{4}He-n scattering. Solid lines, phase-shift analysis of Ref. 31. Dots, "nuclear" ^{4}He-p phase shifts from analysis of Ref. 33. Dashed lines, examples of ND^{-1} results (theoretical S and P phases very sensitive to small changes in input).

I, both a phase shift close to the experimental one (but still too repulsive) and one that is about three times larger can be obtained.

Of particular interest are the $P_{3/2}$ and $P_{1/2}$ phase shifts of n-^{4}He scattering which produce the two lowest ^{5}He resonances. A signature of resonances in ND^{-1} calculations (and in all coupled-channel calculations indeed) is a pronounced minimum in the magnitude of the determinant

$$\|\bar{D}^{J\pi}(E)\| = \det[\bar{D}^{J\pi}_{\alpha\beta}(E)] \tag{4.1}$$

for the particular subspace (J, π) where the resonance is expected. Figure 5 shows the magnitudes of the relevant $\bar{D}$-matrix determinants for $J^\pi = \frac{3}{2}^-$ and $\frac{1}{2}^-$. There is in all cases a minimum in $\|\bar{D}^{3/2^-}\|$ corresponding to the ^{5}He ground state, accompanied by a minimum in $\|\bar{D}^{1/2^-}\|$ at a somewhat higher energy and which corresponds to the first excited state. Qualitatively, these are again the features observed in nature. However, the positions of these minima are again very sensitive, this time to the strength and range of the $^3\mathrm{H} \to d + n$ vertex and to the use or neglect of propagator dressing and virtual s channels in $\bar{B}^{(2)}$. Dependence on the $^4\mathrm{He} \to 3 + 1$ vertex parameters is also there but is much less pronounced. The sensitivity to a vertex that does not occur in the $^4\mathrm{He} + n \to {}^4\mathrm{He} + n$ elements of the driving force, i.e. in lowest order, demonstrates that as expected these resonance minima are largely a result of channel coupling.

Again, in view of this sensitivity no unique result can be given, and the curves of Fig. 5 are to be viewed as just one example. They were obtained with the "standard" parameters from row 5 of Table I, with $P_D = 4\%$, and with Figs. 5(a) and 5(b) corresponding, respectively, to omission and inclusion of s channels and dressing. They also roughly indicate the extreme situations that can be obtained: In the case shown in Fig. 5(b) there is no real ^{5}He ground state but rather a minimum in $\|D^{3/2^-}\|$ at about 16 MeV of $^4\mathrm{He} + n$ separation energy, whereas the first excited state comes as a fairly sharp resonance at some 4 MeV (c.m.) above threshold. More realistic results obtain in the case shown in Fig. 5(a) where the ^{5}He ground state is a resonance at $E^{\mathrm{c.m.}} \approx 4$ MeV (in experiment, $E^{\mathrm{c.m.}}_{\mathrm{res}} \approx 1$ MeV), the first excited state coming a little higher in energy. We may add that by varying $^3\mathrm{H} \to d + n$ vertex parameters, positions of $^5\mathrm{He}_{\mathrm{g.s.}}$ up to about 9 MeV above threshold can be obtained. With $\bar{B}^{(2)}$ omitted, resonances generally come still higher in energy, showing that the $^4\mathrm{He} - n$ force generated by $\bar{B}^{(1)}$ alone is too repulsive.

Moreover, detailed P-wave phase-shift behavior at these resonances, and in particular their almost vanishing widths [$\Gamma \lesssim 50$ keV for the ^{5}He ground state in the case corresponding to Fig. 5(a)], are completely unrealistic. An example, with input again corresponding to the case of Fig. 5(a), is shown in Fig. 4. The abrupt rise of $\delta_{P\,3/2}$ through almost 180° corresponds to the $\|\bar{D}^{3/2^-}\|$ determinant passing slightly below the origin in the complex E plane. (One easily convinces himself that in a two-channel problem at energies below the upper threshold the phase of the $\bar{D}$ determinant is minus the physical scattering phase shift for elastic scattering in the "lower" channel, just as in the single-channel case.) The distance to the origin being extremely small, it is not surprising that slight changes in the input and even inaccuracies of the numerical computation can produce the situation where $\|D^{3/2^-}\|$ passes slightly above the origin and the phase shift therefore abruptly *drops* through almost 180°—a behavior incompatible with the causality limit on $d\delta/dE$.[35] This unrealistic feature in the behavior of $\|\bar{D}\|$ persists when going from $\bar{B} = \bar{B}^{(1)}$ to $\bar{B} = \bar{B}^{(1)} + \bar{B}^{(2)}$ and could not be changed by whatever variation of vertex parameters we tried, so that it is unlikely to come from a neglect of higher-order inputs. It is, moreover, unlikely to come from a neglect of channels to which the resonances couple strongly (which would necessitate the introduction of CDD poles), since other coupled-channel calculations in the $A = 5$ system which also neglect the breakup channels[36,37] have clearly shown that those are quite unessential for the generation of the low-energy P-wave resonances. We conclude that the unrealistic behavior of calculated P-wave phase shifts at these resonances is most probably due to our incorrect treatment of the anomalous threshold of the $^3\mathrm{H}(d,n)^4\mathrm{He}$ pole graph. It should be remembered that this

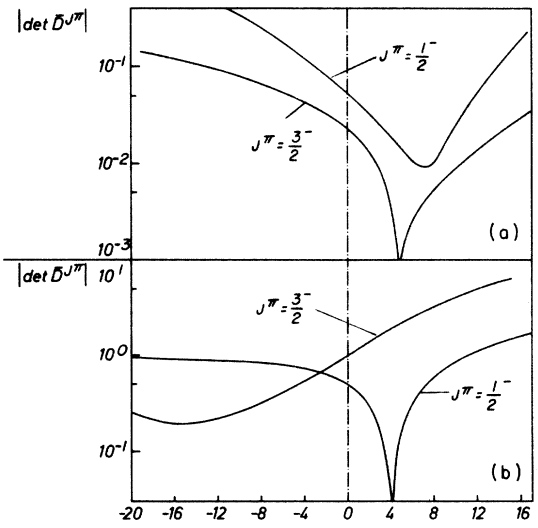

FIG. 5. Absolute magnitudes of $\bar{D}$-matrix determinants for $J^\pi = \frac{1}{2}^-$ and $\frac{3}{2}^-$ as functions of c.m. energy.

graph has an $(E-E_1)^{-(L+1/2)}$ singularity at threshold which may be expected to strongly influence, via channel coupling, the low-energy ^{4}He $+n$ amplitude. It is then plausible that a mistreatment of this analytic structure may cause substantial errors in phase shifts that resonate near threshold. What can be said therefore is that in the present crude form of the theory the *existence* of the P-wave resonances is reproduced, including the $P_{3/2}-P_{1/2}$ spin-orbit splitting, but that their positions are poorly determined, and that realistic widths cannot be obtained.

Attention should be drawn to the fact that the source of projectile-target spin-orbit coupling in this kind of calculation is the existence of at least *one* vertex with a nonvanishing $l>0$ component. Therefore in our case, the spin-orbit splitting between the two $n-^4$He resonances is exclusively due to the D-wave component in the $d \to p+n$ vertex, or, differently stated, to the tensor component in *the nucleon-nucleon interaction*. It is interesting that the sensitivity of those resonances to the accepted range of P_D values is nevertheless modest. Increasing P_D from 4 to 7% results in shifts ~0.5 MeV in the positions with only ~0.1 MeV change in the spin-orbit splitting. Of course, the latter then vanishes if $P_D \to 0$.

Also meriting a special discussion is the $D_{3/2}$ partial wave whose phase shift is generally small in the range of energies covered. The calculated $\|D^{3/2^+}(E)\|$ shows a minimum slightly above the ^{3}H $+d$ threshold, as observed. (It corresponds to the $\frac{3}{2}^+$ second excited "state" of ^{5}He.) It is curious to note that this resonance is not only relatively stable under input variations but that even detailed phase-shift behavior, with its characteristic little kink, is reproduced qualitatively. This result shows that repeated one-cluster exchange for elastic ^{3}H $+d$ scattering is able to generate a qualitatively correct optical potential producing the $\frac{3}{2}^+$ resonance. This resonance is obviously far enough in energy ($E_{\text{c.m.}} \approx 18$ MeV) from the $n+^4$He threshold to remain unaffected by our crude approximate treatment of the anomalous threshold.

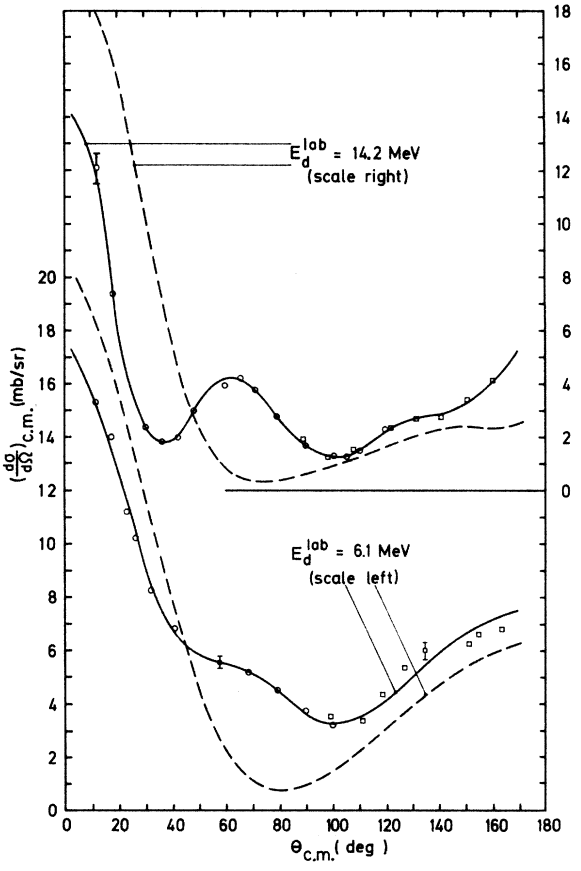

FIG. 6. Unpolarized c.m. differential cross sections for the ^{3}H(d,n) ^{4}He process at two deuteron energies. Circles, experimental points; squares, ^{3}He(d,p) ^{4}He measurements; solid lines, Legendre-polynomial fits to measurements; all from Ref. 38. Dashed lines, ND^{-1} results.

B. Deuteron stripping on the triton

Calculated differential cross sections for the ^{3}H$(d,n)^4$He transfer process, at two different deu-

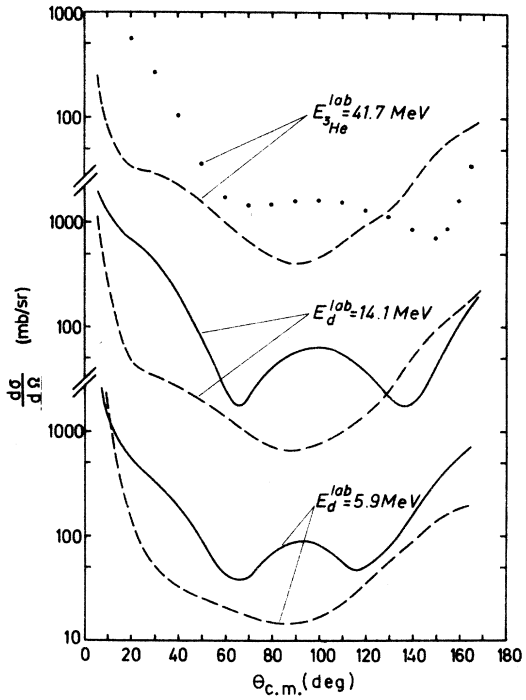

FIG. 7. Unpolarized c.m. differential cross sections for ^{3}H $+d$ elastic scattering. Solid lines, experimental values from Ref. 39; squares, ^{3}He $+d$ measurements from Ref. 40. Dashed lines, ND^{-1} results.

teron energies, are compared with experiment[38] in Fig. 6. (The cross sections of Figs. 6 and 7 were calculated from partial waves up to and including $J=\frac{11}{2}$.) Absolute magnitudes in both the forward and backward maxima are reasonably good. On the other hand, the smaller maximum at medium angles is missing—in the framework described here it could not be produced with any of the acceptable sets of subsystem parameters. The same defect will be seen to occur in $^3\mathrm{H}+d$ elastic scattering cross sections. Since there are indications (although at present no really conclusive experimental evidence) of the existence of several broad resonances with almost pure $L=2$ $^3\mathrm{H}+d$ cluster structure around 5 MeV (c.m.) above the $^3\mathrm{H}+d$ threshold[33,46] it is tempting to speculate that the smaller maximum in medium energy $^3\mathrm{H}(d,n)^4\mathrm{He}$ cross sections might arise from $L=2$ initial-state interaction through those resonances. At the moment we must admit ignorance about precisely what deficiency of our input is responsible for the failure to obtain this effect. It is certainly possible that the neglect of the "crossed" stripping graph in Fig. 1(b) is not justified, and parameter determinations for the $^4\mathrm{He}\to d+d$ vertex would therefore be welcome. We still feel that, otherwise, the theoretical curves of Fig. 6 are encouraging.

In the energy region above the $^3\mathrm{H}+d$ threshold, the physical quantities studied here are generally speaking much less dependent on changes in the input than the extremely sensitive $^4\mathrm{He}+n$ phase shifts at low energies. The $\frac{3}{2}^+$ resonance was already mentioned. Also, the theoretical transfer cross sections in Fig. 6 (calculated with the "standard" parameter values of Table I, with s channels and propagator dressing in $\bar{B}^{(2)}$, and with $P_D=4\%$) can be changed in magnitude by some 20% when varying $t\to d+n$ or $^4\mathrm{He}\to 3+1$ vertex parameters, or switching off propagator dressing and s channels, but the angular shape always remains the same. We note, however, that here second-order inputs are essential for obtaining the correct rise at backward angles—with $\bar{B}=\bar{B}^{(1)}$, that rise is there but always too weak.

C. Triton-deuteron elastic scattering

We are not aware of the existence of any detailed phase-shift analysis for elastic $^3\mathrm{H}+d$ scattering. Figure 7 therefore directly compares theoretical $^3\mathrm{H}(d,d)^3\mathrm{H}$ angular distributions at three sample energies with experiment.[39] For the highest energy of $E^{\mathrm{c.m.}}=34.2$ MeV ($=E_2+16.6$ MeV), we have plotted as experimental data a $^3\mathrm{He}+d$, rather than a $^3\mathrm{H}+d$, cross section[40]—since experimentally those two quantities are found to be nearly identical (except at very small angles) at the lower energies,[39] this should not make a difference for our purpose.

Again, a smaller maximum at medium angles is missing, as discussed in connection with the stripping process. More importantly, cross sections at forward angles come out much too small. Once more, this angular pattern is fairly stable under variations of the input. A closer look at the results shows that the calculated "nuclear" amplitudes at the forward angles are quite small so that cross sections are mainly given by the rapidly decreasing Rutherford cross section, whereas the experimental values are up to 10 times as large. By contrast, the strong backward peaking is reproduced reasonably well.

A somewhat puzzling result is that these cross sections do not improve appreciably when going from first order to first-plus-second order inputs. This fact may be accidental, and it certainly does not exclude the possibility of higher order inputs still being important. In view of the weak binding of the deuteron projectile, which above $E^{\mathrm{c.m.}}=E_2+2.23$ MeV should lead to rather frequent three-body breakup, we moreover suspect that as far as $^3\mathrm{H}+d$ elastic scattering is concerned, Eq. (2.15) is no more an acceptable approximation.

5. DISCUSSION AND CONCLUSION

We produced above results of an ND^{-1} calculation of elastic and transfer reactions between two clusters with total $A=5$. The theory stresses two-cluster unitarity, simple analytic structure, and cluster exchanges (single and double) as driving mechanism. As a consequence one could describe the processes and their coupling as repeated cluster exchange.

It hardly needs emphasis that with the simple assumptions and approximations underlying our calculations, as spelled out above, one cannot expect accurate agreement with experiment to result. However, the additional labor required to treat unitarity defects,[20] anomalous thresholds,[29] or higher order inputs, is considerable. Our primary interest therefore has been to test the theory in its simplest approximation.

The outcome may be summarized as follows. For the elastic scatterings calculated quantities show a crude similarity, and sometimes order-of-magnitude agreement, with experiment, except for the widths of P-wave neutron-α resonances where the present simplified form of the theory fails. Among the details that are unsatisfactory, the more serious ones are the positions of P-wave resonances, which are ill-determined positions due to violent dependence on input, and further the bad forward amplitudes for $^3\mathrm{H}+d$ scattering.

Transfer cross sections, except for some finer detail of their angular pattern, agree well with the measurements, showing that for this process pole and box diagrams when unitarized through a coupled-channel ND^{-1} scheme provide a basically sound description of the reaction mechanism.

We reemphasize at this point that we deliberately refrain from using the existing uncertainties in subsystem parameters to perform any "best fits" to the data. An "agreement" produced by parameter fitting would make little sense since omitted refinements would change those fitted values. More seriously, a parameter readjustment with the purpose of improving results for one channel is incompatible with the ND^{-1} formalism which aims at a prediction of *all* A-particle observables from the *same* set of quantities related to subsystems.

Having mentioned above explicit deficiencies in our application of the ND^{-1} method we wish to further comment on two of these in view of recent investigations. Kok, Greben, and van der Ploeg[49] performed model studies of potential scattering, applying the standard one-channel N/D method. They concluded that for large coupling constants one needs driving terms up to $\bar{B}^{(4)}$ in order to get satisfactory agreement with the known, exact solution. In a "realistic" many-channel problem, numerical convergence studies using higher order input would be difficult, but we may expect by analogy that those higher terms will be important at least for the ^{4}He-n elastic amplitude where appreciable changes occur when going from $\bar{B}^{(1)}$ to $\bar{B}^{(1)}$ to $\bar{B}^{(2)}$, and perhaps also for the $^3\mathrm{H}+d$ processes.

The Groningen group further succeeded in incorporating the singularity structure of anomalous thresholds into the ND^{-1} framework[29] and we understand that a more complete treatment of the $A=5$ system is part of their program.

Inclusion of this point could influence some of our results. For instance, the P-wave resonances in elastic n-^{4}He scattering, being relatively close to threshold, will be sensitive to the anomalous threshold of the $^3\mathrm{H}(d,n)\,^4$He pole graph. Our approximate account of this effect clearly cannot provide more than a crude estimate. In particular, we conjecture that realistic ^{5}He widths cannot be obtained without a proper treatment of the anomalous threshold. The appearance of such anomalies, and the considerable increase in effort required to take them correctly into account, constitute an undeniable disadvantage of the dispersion approach.

But whatever the influence of anomalous thresholds it is actually gratifying to see ordered resonances emerge from a microscopic theory as opposed to a semiphenomenological approach using an effective optical potential. The situation may be compared with, e.g., a shell-model reaction theory[41] where reasonable *gross* positions of such single-particle resonances are ensured by a suitable choice of the basic one-body potential for the total A-particle system. A corresponding procedure in the ND^{-1} framework would be to analyze the total input matrix so as to explicitly display and extract gross positions of bound states or resonances of the total reacting system. These could then be replaced with their experimental values, with the remainder input producing shifts and widths only. While technically such a program could be implemented with the already mentioned CDD-pole prescription of Ref. 18, it would clearly represent another departure from the strict philosophy emphasized before.

Closest in spirit to the ND^{-1} method are generalizations of the Faddeev theory, in particular with respect to the driving terms. In practice, however, the theories are utterly different and are beset by specific mathematical difficulties. Offhand it would seem that the solution of singular Faddeev type equations is of lower complexity than for instance the anomalous thresholds problem. In practice we know of one application to $A=4$,[42] with rather limited success, while a treatment of the five-nucleon problem parallel to the ND^{-1} treatment is in progress.

We are not aware of other dispersion calculations regarding the $A=5$ system. For a discussion of graph methods as well as of procedures using K-matrix unitarization of some input, we refer to Refs. 43 and 44.

Next we turn to a comparison with variational coupled-channel theories of light systems such as the resonating-group method[10] or the Kohn-Hulthén formalism of Hackenbroich and Heiss.[11] Both methods have found successful application to the five-nucleon system.[37,45,46] Here the ^{5}He and ^{5}Li work of Heiss and Hackenbroich may be termed a true *ab-initio* calculation since both the internal wave functions of the subsystems and the reactions between them are calculated from one and same semiempirical two-nucleon force, excluding any adjustable or phenomenological input. As in the present work, coupling to breakup channels is generally neglected. (An exception is Ref. 46 where a $^4\mathrm{He}^*+p$ pseudochannel was introduced for the specific purpose of obtaining certain conjectured odd-parity ^{3}He-d resonances.) The method produces good S and P wave $^4\mathrm{He}+n$ phase shifts[37] and is clearly superior to the ND^{-1} results produced here. With regard to the $\frac{3}{2}^+$ "threshold" resonance, the two methods appear to be doing about equally well, while for the two $^3\mathrm{H}+d$ processes comparison is difficult because Refs. (37)

and (46) report on phases of S-matrix elements rather than differential cross sections. Instead we may look at the ^{3}He$(d, p)\alpha$ and ^{3}He$(d, d)^3$He cross sections of Chwieroth *et al.*[45] whose resonating-group calculation is similar in spirit to that of Ref. 46. Calculated angular distributions and in particular small-angle elastic cross sections show closer agreement with the data than our predictions. On the other hand the calculations use phenomenological imaginary parts for the elastic scattering potentials, and at present it is not easy to judge to what extent the good absolute values of the cross sections depend on the introduction of these imaginary parts. A meaningful comparison with the results described in this paper is therefore again difficult.

To a much higher degree, the latter statement applies to a comparison with the coupled Schrödinger equation model of de Facio, R. K. Umerjee, and J. L. Gammel[36] where phenomenological potentials fitted to the elastic scatterings are used and the nondiagonal (coupling) part of the potential matrix is adjusted in each partial wave so as to produce the experimental reaction cross section. While this method produces highly accurate parametrizations (preserving the coupled-channel aspect) of almost all observable five-nucleon quantities, it is evidently too different in both its aim and starting point to be compared to calculations deriving those observables from nonadjustable *subsystem* parameters.

In spite of its apparent inferiority we feel that the ND^{-1} method should be further exploited.[29] Our major argument is based on the fact that with variational calculations in general little insight is acquired as regards the reaction mechanism. In contradistinction, a pursuit of an improved ND^{-1} investigation will ultimately tell whether the repeated exchange mechanism is really dominant or not in a general sense. We feel that the exploratory results reported here justify such an effort.

We acknowledge discussions with J. Hüfner, L. P. Kok, and D. E. Atkinson. H. G. Beisenherz kindly drew our attention to the paper by Kinoshita. M. S. would like to offer belated thanks to H. J. Mang and W. Wild for the hospitality extended to him in 1970/71 at Munich Technical University where work on the Pagels ND^{-1} computer code was started.

Program testing was largely done on the TR 4 and TR440 Telefunken computers of the Leibniz computer center at Munich. Final tests and actual computations were carried out on the UNIVAC 1106 of the University of Freiburg. The cooperation of both institutions is acknowledged.

APPENDIX A: DETERMINATION OF PAGELS PARAMETERS

In choosing pole positions a and residues r for the Pagels approximation (2.18) we adopt, with slight modifications necessary for a nonrelativistic problem the Padé criterion as applied to the present problem by Sweig.[47] Using the variable

$$w = w(E) = \frac{E - E_F}{E_C - E}, \tag{A1}$$

where the "fitting-point energy"

$$E_F = E_F(C, L) < E_C \tag{A2}$$

may in principle be chosen differently for each (C, L), we write the right-hand spectral integral (2.17), with cutoff (2.21), as

$$\bar{R}_{C,L}(E, E_p, E_U) = f_{C,L}(E_p, E_U)\,\frac{E_C - E_F}{E_C - E}\,\Omega_{C,L}(w, E_p, E_U, E_F) \tag{A3}$$

where

$$f_{C,L}(E_p, E_U) = \left[\frac{2M_C}{\hbar^2(E_C - E_p)}\right]^{3/2}\left[\frac{2M_C}{\hbar^2}\,(E_U - E_C)\right]^{L}. \tag{A4}$$

The remaining, dimensionless, integral

$$\Omega_{C,L}(w, E_p, E_U, E_F) = \int_0^1 \frac{\sigma_{C,L}(E'(x, E_F), E_p, E_U)}{(1 - x)(1 + wx)}\,dx \tag{A5}$$

is a "series of Stieltjes" in w.[47] Here,

$$\sigma_{C,L}(E', E_p, E_U) = \bar{\rho}_{C,L}(E')\left\{f_{C,L}(E_p, E_U)\,(E' - E_p)^2\left[1 - \delta_{L0} + \left(\frac{E' - E_C}{E_U}\right)^{L}\right]\right\}^{-1} \tag{A6}$$

and

$$E'(x, E_F) = E_C + \frac{x}{1 - x}\,(E_C - E_F). \tag{A7}$$

The $[N, M]$ Padé approximants of (A5) at $w = 0$ may be obtained in a standard fashion.[48] We refer the reader to Ref. 47 for a discussion of why approximating Ω is preferable over a direct approximation of $\bar{R}$.

According to general Padé theory,[48] for given N the $M=N$ and $M=N-1$ approximants are the ones that provide, respectively, the best upper and lower bounds on $\Omega(w)$. Since from (A3)

$$\Omega_{C,L} \to 0 \quad \text{as } E \to E_C \text{ (i.e., as } w \to \infty), \tag{A8}$$

the choice $M=N-1$ is indicated. We therefore calculate, by the usual Padé algebra,[48] the coefficients μ_n and ν_n in

$$\Omega_\alpha(w) \approx \left[\sum_{n=0}^{n_p-1} \mu_{\alpha,n} w^n\right] \left[\sum_{n=0}^{n_p-1} \nu_{\alpha,n} w^n + w^{n_p}\right]^{-1}, \tag{A9}$$

where we wrote n_p instead of N. This requires knowledge of the first $2\times n_p$ Taylor coefficients of (A5) at $w=0$ which are evaluated by numerical quadrature. Note that these coefficients depend on E_p, E_U, and E_F. For most cases they can be worked out analytically but the resulting expressions have rather sensitive cancellations built in and are therefore not suitable for calculations. On the other hand, since their integrands are smooth, positive-definite functions, accurate numerical evaluations are quite easy to perform.

It then remains to establish the pole-sum form of Eq. (2.18) whose parameters are needed for Eqs. (2.19). For that purpose one performs a partial-fraction decomposition, writing (A9) in the form

$$\sum_{n=1}^{n_p} \frac{\gamma_n(E_p, E_U, E_F)}{w - \eta_n(E_p, E_U, E_F)}, \tag{A10}$$

where

$$\gamma_n = \left[\sum_{m=0}^{n_p-1} \mu_m(\eta_n)^m\right] \left[\sum_{m=1}^{n_p-1} m\nu_m(\eta_n)^{m-1} + n_p(\eta_n)^{n_p-1}\right]^{-1} \tag{A11}$$

and where the η_n $(n=1, 2, \ldots n_p)$ are the zeros of the denominator polynomial in (A9) which again are determined numerically. According to Padé theory[48] they are all real, negative, and distinct.

Inserting (A10) into (A3) one finally obtains the desired form (2.18) where

$$a_{\alpha,n} \equiv a_{CLn}(E_p, E_U, E_F) = E_C + \frac{E_C - E_F}{-1 - \eta_{CLn}(E_p, E_U, E_F)}, \tag{A12a}$$

$$\gamma_{\alpha,n} \equiv \gamma_{CLn}(E_p, E_U, E_F) = f_{CL}(E_p, E_U) \frac{(E_C - E_F)\gamma_{CLn}(E_p, E_U, E_F)}{-1 - \eta_{CLn}(E_p, E_U, E_F)}. \tag{A12b}$$

By construction the approximation becomes exact at $E=E_F$, the fitting energy.

APPENDIX B: COULOMB EFFECTS IN DRIVING FORCES

The reader may have noticed that the pole and box graphs of Figs. 1 and 2 actually represent contributions to certain *unreduced* amplitudes *without* Coulomb effects. However, in Sec. 3 they were tacitly used as Born terms for the *Coulomb-reduced* amplitudes $\bar{A}$ of Eq. (2.5). This Appendix serves to explain that procedure and to point out the approximations inherent in it.

The general prescription for obtaining the left-hand discontinuities of reduced amplitudes[18] reads

$$\mathrm{Im}\bar{B}_{\alpha\beta} = d_\alpha^* \mathrm{Im}[B_{\alpha\beta} - \delta_{\alpha\beta} B_\alpha^{\mathrm{Coul}}] d_\beta, \tag{B1}$$

where the star on d_α may actually be omitted since the middle factor is nonzero only on the left where d_α is real. On the other hand, using the Gell-Mann Goldberger transformation we may write (omitting angular momentum projection)

$$\mathrm{Im}[B_{\alpha\alpha'} - \delta_{\alpha\alpha'} B_\alpha^{(\mathrm{Coul})}] = \mathcal{P}_L \left\{ \left\langle \varphi_\alpha^- \middle| \bar{V}_C - U_C^{(\mathrm{Coul})} + (\bar{V}_C - U_C^{(\mathrm{Coul})}) \frac{1}{E + i\epsilon - H} (\bar{V}_{C'} - U_{C'}^{(\mathrm{Coul})}) \middle| \varphi_{\alpha'}^+ \right\rangle \right\}, \tag{B2}$$

where $\bar{V}_C$ denotes the channel interaction and $U_C^{(\mathrm{Coul})}$, the point-charge Coulomb potential between the two fragments in channel C, and where $|\phi_\alpha^\pm\rangle$ are Coulomb-distorted channel wave functions describing relative fragment motion in C under the influence of $U_C^{(\mathrm{Coul})}$ only.

In the spirit of approximation (2.15) we next replace the exact Green's function by its projection onto the space of exact two-fragment scattering states $|\Psi_\alpha^+\rangle$ and eventually of bound states $|\Psi_B\rangle$, omitting all scattering states of a breakup type. This turns (B2) into the expression

$$\mathcal{P}_L \left\{ \left\langle \varphi_\alpha^- \middle| (\bar{V}_C - U_C^{(\mathrm{Coul})}) + (\bar{V}_C - U_C^{(\mathrm{Coul})}) \left[\sum_B \frac{|\Psi_B\rangle\langle\Psi_B|}{E - E_B} + \sum_{\alpha''} \int_{E_{C''}}^\infty \rho_{\alpha''}(E'') \frac{|\Psi_{\alpha''}^+(E'')\rangle\langle\Psi_{\alpha''}^+(E'')|}{E + i\epsilon - E''} dE'' \right] \times (\bar{V}_{C'} - U_{C'}^{(\mathrm{Coul})}) \middle| \varphi_{\alpha'}^+ \right\rangle \right\}. \tag{B3}$$

The approximations leading to our choice of input are then the following:

(i) Assume that for all two-fragment channels C

$$\bar{V}_C - U_C^{(\mathrm{Coul})} \approx \bar{V}_C^{(N)} , \tag{B4}$$

the purely nuclear channel interaction. Physically this amounts to neglecting the finite extension and the "granular" single-proton structure of fragment charge distributions.

(ii) Replace

$$|\varphi_\alpha^\pm\rangle \approx [d_\alpha(E \pm i\epsilon)]^{-1} |\alpha_1 E\rangle , \tag{B5a}$$

where $|\alpha\rangle$ is the usual channel wave function with *free* relative motion. From the definition of a Jost function, this would be exact at zero fragment distance $|\vec{R}_C|$. This over-all description of Coulomb distortion by a complex depletion factor therefore means to assume that the range of nuclear forces $\bar{V}_C^{(N)}$ acting on the $|\phi_\alpha^\pm\rangle$ in Eq. (B3) is very short.

To be consistent, one should then put in the spectral integral

$$|\Psi_\alpha^+(E)\rangle \approx [d_\alpha(E+i\epsilon)]^{-1} |\Psi_\alpha^{+(N)}(E)\rangle , \tag{B5b}$$

with $|\Psi_\alpha^{+(N)}\rangle$ the exact scattering state produced by the purely nuclear channel interaction (B4). This essentially amounts to neglecting the mutual *Coulomb* polarization of fragment charge distributions.

(iii) Neglect Coulomb effects in $|\Psi_B\rangle$. The resulting approximate expression

$$d_\alpha^{-1} \mathcal{P}_L \left\{ \left\langle \alpha, E \middle| \bar{V}_C^{(N)} + \sum_B \frac{\bar{V}_C^{(N)} |\Psi_B^{(N)}\rangle \langle \Psi_B^{(N)}| \bar{V}_{C'}^{(N)}}{E - E_B} \right.\right.$$

$$\left.\left. + \sum_{\alpha''} \int_{E_{C''}}^{\infty} \bar{\rho}_{\alpha''}(E'') \frac{\bar{V}_C^{(N)} |\Psi_{\alpha''}^{+(N)}(E'')\rangle \langle \Psi_{\alpha''}^{+(N)}(E'')| \bar{V}_{C'}^{(N)}}{E + i\epsilon - E''} dE'' \middle| \alpha', E \right\rangle \right\} d_{\alpha'}^{-1} , \tag{B6}$$

contains Coulomb effects—except for the d^{-1} factors which disappear when inserting into (B1)—only in the internal fragment wave functions in $|\alpha\rangle$ and $|\alpha'\rangle$ and in the occurrence of the modified phase-space matrix $\bar{\rho}$ of Eq. (2.13). The "undistorted" pole and box graphs we used here are then the first- and second-order Born terms corresponding to the last-written driving force.

*Work partly supported by Deutsche Forschungsgemeinschaft.

†Present address: Institut für Theoretische Physik I der Universität Münster, D-4400 Münster, Von-Esmarch-Strasse 10 a, West Germany.

[1]L. D. Faddeev, Zh. Eksperim. i Teor. Fiz. 39, 1459 (1960) [transl.: Sov. Phys.—JETP 12, 1014 (1961)].

[2]A. N. Mitra, Nucl. Phys. 32, 529 (1962); A. G. Sitenko and V. F. Kharchenko, Yad. Fiz. 1, 994 (1965) [transl.: Sov. J. Nucl. Phys. 1, 708 (1965)]; R. Aaron, R. D. Amado, and Y. Y. Yam, Phys. Rev. 140, B1291 (1965); A. C. Phillips, Phys. Lett. 20, 50 (1966); Phys. Rev. 142, 984 (1966).

[3]W. M. Kloet and J. A. Tjon, Phys. Lett. 37B, 460 (1971); Ann. Phys. (N.Y.) 79, 407 (1973).

[4]L. M. Delves and A. C. Phillips, Rev. Mod. Phys. 41, 497 (1969).

[5]W. Ebenhöh, Nucl. Phys. A191, 97 (1972).

[6]E.g., O. Zohni, Phys. Rev. C 8, 1164 (1973).

[7]W. E. Meyerhof and T. A. Tombrello, Nucl. Phys. A109, 1 (1968); T. Lauritsen and F. Ajzenberg-Selove, Nucl. Phys. 78, 1 (1966).

[8]O. A. Yakubowski, Yad. Fiz. 5, 1312 (1967) [transl.: Sov. J. Nucl. Phys. 5, 937 (1967)]; Y. Avishai, Nucl. Phys. A150, 379 (1970); E. O. Alt, G. Grassberger, and W. Sandhas, Nucl. Phys. B2, 181 (1967); I. H. Sloan, Phys. Rev. C 6, 1945 (1972).

[9]I. M. Narodetski and O. A. Yakubowski, Yad. Fiz. 14, 315 (1971) [transl.: Sov. J. Nucl. Phys. 14, 178 (1972)].

[10]E.g., Y. C. Tang, in *Proceedings of the International Conference on Clustering Phenomena in Nuclei, Bochum, Germany, 21–24 July, 1969* (International Atomic Energy Agency, Vienna, Austria, 1969), p. 109.

[11]H. H. Hackenbroich and P. Heiss, Z. Phys. 231, 216, 225 (1970); P. Heiss and H. H. Hackenbroich, *ibid.* 235, 422 (1970).

[12]T. E. O. Ericson and M. P. Locher, Phys. Lett. 27B, 576 (1968); Nucl. Phys. A148, 1 (1970).

[13]A. S. Rinat (Reiner) and M. Stingl, Ann. Phys. (N.Y.) 65, 141 (1971).

[14]G. Barton and A. C. Phillips, Nucl. Phys. A132, 97 (1969); Y. Avishai, W. Ebenhöh, and A. S. Rinat (Reiner), Ann. Phys. (N.Y.) 55, 341 (1969); M. Kac, Ann. Phys. (N.Y.) 81, 113 (1973).

[15]R. H. J. Bower, Ann. Phys. (N.Y.) 73, 372 (1972).

[16]R. Blankenbecler *et al.*, Ann. Phys. (N.Y) 10, 62 (1960).

[17]A. S. Rinat (Reiner), L. P. Kok, and M. Stingl, Nucl. Phys. A190, 328 (1972).

[18]M. Kugler, Phys. Rev. 146, 1026 (1966); K. Kinoshita, Prog. Theor. Phys. 38, 705 (1967).

[19]J. D. Bjorken, Phys. Rev. Lett. 4, 473 (1960); R. L. Warnock, Nuovo Cimento 50A, 894 (1967).

[20]R. L. Warnock, Phys. Rev. 146, 1109 (1966).

[21]H. Pagels, Phys. Rev. 140, B1599 (1965).
[22]L. Castillejo, R. H. Dalitz, and F. J. Dyson, Phys. Rev. 101, 453 (1956).
[23]M. Stingl and A. S. Rinat (Reiner), Nucl. Phys. A154, 613 (1970).
[24]A. C. Phillips, Nucl. Phys. A107, 209 (1968).
[25]Reference 26 contains some new determinations of the $^3H \rightarrow d + n$ coupling constant, all essentially agreeing with the figure given in Table II (the corresponding value of the quantity C^2 used in those papers is ~3.4).
[26]L. J. B. Goldfarb, J. A. Gonzalez, and A. C. Phillips, Nucl. Phys. A209, 77 (1973); Y. E. Kim and A. Tubis, Phys. Rev. Lett. 29, 1017 (1972); T. K. Lim, Phys. Rev. Lett. 30, 709 (1973).
[27]E. P. Harper, Y. E. Kim, and A. Tubis, Phys. Rev. Lett. 28, 1533 (1972).
[28]G. R. Plattner *et al.*, Nucl. Phys. A206, 513 (1973).
[29]J. M. Greben and L. P. Kok, unpublished.
[30]S. Mandelstam, Phys. Rev. Lett. 4, 84 (1959).
[31]R. A. Arndt and L. D. Roper, Phys. Rev. C 1, 903 (1970).
[32]R. A. Arndt, D. D. Lang, and L. D. Roper, Nucl. Phys. A209, 429 (1973); R. A. Arndt and L. D. Roper, *ibid.*, 447 (1973).
[33]G. R. Plattner, A. D. Bacher, and H. E. Conzett, Phys. Rev. C 5, 1158 (1972).
[34]P. Swan, Proc. Roy. Soc. 228, 10 (1955).
[35]E.g., R. G. Newton, *Scattering Theory of Waves and Particles* (McGraw Hill, New York, 1966), p. 314.
[36]B. de Facio, R. K. Umerjee, and J. L. Gammel, Phys. Rev. 151, 819 (1966), Phys. Lett. 25B, 449 (1967).
[37]P. Heiss and H. H. Hackenbroich, Z. Phys. 231, 230 (1970).
[38]L. Stewart, J. E. Brolley, Jr., and L. Rosen, Phys. Rev. 119, 1649 (1960).
[39]J. E. Brolley *et al.*, Phys. Rev. 117, 1307 (1960).
[40]T. R. King and R. Smythe, Nucl. Phys. A183, 657 (1972).
[41]C. Mahaux and H. A. Weidenmüller, *Shell Model of Nuclear Reactions* (North-Holland, Amsterdam, 1969).
[42]E. O. Alt, P. Grassberger, and W. Sandhas, Phys. Rev. C 1, 85 (1971).
[43]I. Borbei, E. I. Dolinskii, and V. V. Turovtsev, Yad. Fiz. 8, 492 (1968) [transl.: Sov. J. Nucl. Phys. 8, 287 (1969)].
[44]J. Kraus and K. L. Kowalski, Phys. Rev. C 2, 1319 (1972); A. G. Baryshnikov *et al.*, Zh Eksperim. i Teor. Fiz. Pis'ma Red. 16, 414 (1972) [transl.: Sov. Phys.— JETP Lett. 16, 294 (1972)].
[45]F. S. Chwieroth *et al.*, Phys. Rev. C 8, 938 (1973).
[46]P. Heiss and H. H. Hackenbroich, Phys. Lett. 30B, 373 (1969); Nucl. Phys. A162, 530 (1971).
[47]M. J. Sweig, Phys. Rev. 165, 1893 (1968).
[48]G. A. Baker, Jr., in *Advances in Theoretical Physics*, edited by K. A. Brueckner (Academic, New York, 1965), Vol. I.
[49]L. P. Kok, J. M. Greben, and F. A. van der Ploeg, Ann. Phys. (N.Y.) 79, 386 (1973).